

This discussion paper is/has been under review for the journal Atmospheric Chemistry and Physics (ACP). Please refer to the corresponding final paper in ACP if available.

# Explicit modeling of volatile organic compounds partitioning in the atmospheric aqueous phase

C. Mouchel-Vallon<sup>1</sup>, P. Bräuer<sup>2</sup>, M. Camredon<sup>1</sup>, R. Valorso<sup>1</sup>, S. Madronich<sup>3</sup>, H. Herrmann<sup>2</sup>, and B. Aumont<sup>1</sup>

<sup>1</sup>Laboratoire Interuniversitaire des Systèmes Atmosphériques, CNRS/INSU UMR7583, Université Paris Est Créteil et Université Paris Diderot, Institut Pierre Simon Laplace, 94010, Créteil, France

<sup>2</sup>Leibniz-Institut für Troposphärenforschung, Permoserstr. 15, 04318 Leipzig, Germany

<sup>3</sup>NCAR, National Center for Atmospheric Research, Boulder, Colorado, USA

Received: 14 August 2012 – Accepted: 5 September 2012 – Published: 14 September 2012

Correspondence to: B. Aumont (bernard.aumont@lisa.u-pec.fr)

Published by Copernicus Publications on behalf of the European Geosciences Union.

## Abstract

The gas phase oxidation of organic species is a multigenerational process involving a large number of secondary compounds. Most secondary organic species are water-soluble multifunctional oxygenated molecules. The fully explicit chemical mechanism 5 GECKO-A (Generator of Explicit Chemistry and Kinetics of Organics in the Atmosphere) is used to describe the oxidation of organics in the gas phase and their mass transfer to the aqueous phase. The oxidation of three hydrocarbons of atmospheric interest (isoprene, octane and  $\alpha$ -pinene) is investigated for various  $\text{NO}_x$  conditions. The simulated oxidative trajectories are examined in a new two dimensional space defined by the mean oxidation state and the solubility. The amount of dissolved organic 10 matter was found to be very low (< 2 %) under a water content typical of deliquescent aerosols. For cloud water content, 50 % (isoprene oxidation) to 70 % (octane oxidation) of the carbon atoms are found in the aqueous phase after the removal of the parent hydrocarbons for low  $\text{NO}_x$  conditions. For high  $\text{NO}_x$  conditions, this ratio is only 5 % in 15 the isoprene oxidation case, but remains large for  $\alpha$ -pinene and octane oxidation cases (40 % and 60 %, respectively). Although the model does not yet include chemical reactions in the aqueous phase, much of this dissolved organic matter should be processed in cloud drops and modify both oxidation rates and the speciation of organic species.

## 1 Introduction

20 The atmospheric aqueous phase includes water in clouds and fogs droplets and deliquescent particles. There is a lack of knowledge concerning the aqueous phase contribution to the atmospheric chemistry (Ravishankara, 1997). Inorganic compounds reactivity in atmospheric water and their contribution to particulate matter formation has been extensively studied (e.g. Finlayson-Pitts and Pitts, 2000; Kreidenweis et al., 2003; 25 Monod and Carlier, 1999). However large uncertainties still remain about the fate of dissolved organics. Most secondary organic species are water-soluble multifunctional

ACPD

12, 24095–24130, 2012

## Explicit modeling of volatile organic compounds

C. Mouchel-Vallon et al.

[Title Page](#)

[Abstract](#)

[Introduction](#)

[Conclusions](#)

[References](#)

[Tables](#)

[Figures](#)

◀

▶

◀

▶

[Back](#)

[Close](#)

[Full Screen / Esc](#)

[Printer-friendly Version](#)

[Interactive Discussion](#)



oxygenated species. Because gas phase oxidation mechanisms are unable to reproduce experimental secondary organic aerosol (SOA) yields (Carlton et al., 2009; Ervens et al., 2011; Hallquist et al., 2009), aqueous phase mediated SOA formation is currently studied as a way to enhance aerosol yields (Carlton et al., 2009; El Haddad et al., 2009; Ervens and Volkamer, 2010; Ervens et al., 2008, 2011; Fu et al., 2009; Hallquist et al., 2009).

The study of aqueous phase chemistry as a potential source of SOA has shown that oxidation in water of secondary species could contribute to SOA mass. For example, Lim et al. (2005) have shown in a modeling study that the cloud oxidation of 10 aldehydes originating from isoprene oxidation could be responsible for 4–20 % of the total isoprene SOA yield. Similarly, Myriokefalitakis et al. (2011) have shown that cloud chemistry could enhance oxalate production by  $2 \text{ Tg yr}^{-1}$ , a contributor to SOA mass. Ervens and Volkamer (2010) modeled the SOA formation through aqueous phase processing of glyoxal, one of the oxidation products of isoprene, and have confirmed that 15 there is a correlation between SOA mass increase and the liquid water content ( $L$ ). Biogenic terpenes SOA yields from gas phase photo-oxidation have been explored in detail (e.g. Hallquist et al., 2009). Several recent experimental works have studied the influence of aqueous phase photooxidation on the composition of SOA formed after oxidation of biogenic compounds (Lee et al., 2011, 2012; Bateman et al., 2011). As 20 for anthropogenic hydrocarbons, several recent studies have measured (Lim and Ziemann, 2005; Russell et al., 2011) or modeled (Jordan et al., 2008; Aumont et al., 2012) the gas phase SOA yields of alkanes. Recent experimental results from Zhou et al. (2011) suggest that SOA yields of four aromatic hydrocarbons (toluene and xylenes) are correlated to the ambient liquid water.

25 The mechanism of volatile organic compound (VOC) processing by the aqueous phase can be split in two steps:

- i. Phase partitioning. Specifically, many secondary organic species formed during the gas phase oxidation of hydrocarbons are highly soluble and are thus expected

[Title Page](#)[Abstract](#)[Introduction](#)[Conclusions](#)[References](#)[Tables](#)[Figures](#)[◀](#)[▶](#)[◀](#)[▶](#)[Back](#)[Close](#)[Full Screen / Esc](#)[Printer-friendly Version](#)[Interactive Discussion](#)

to be found in atmospheric water (e.g. Aumont et al., 2000; van Pinxteren et al., 2005).

- ii. Aqueous phase reactivity. Like in the gas phase, dissolved compounds are oxidized by radicals in water, mainly by OH and NO<sub>3</sub> (Herrmann, 2003; Warneck, 2005). Resulting products are similar to those observed in the gas phase, but rate constant are generally faster and the yields of the various products are substantially modified (Herrmann, 2003). Moreover in the aqueous phase, hydration and acid dissociation can occur, which lead to the formation of some organic products (hydrates and carboxylate ions) not formed in the gas phase. Additional processes forming heavier species can occur in the aqueous phase, like esterification and aldol condensation (e.g. Nguyen et al., 2011; Altieri et al., 2008).

As experimental studies inside clouds are scarce and very difficult to set up (Crahan et al., 2004; Herrmann et al., 2005; Sorooshian et al., 2007), most of the organics clouds chemistry studies have been performed based on modeling approaches. These models usually represent the condensed phase as a single well mixed aqueous phase in which organic species undergo oxidation. This aqueous oxidation scheme is coupled with specifically tailored gas phase mechanisms taking into account mass transfer between the two phases (e.g. Jacob, 1986; Barth et al., 2003; Lelieveld and Crutzen, 1991; Leriche et al., 2000; Ervens et al., 2008; Tilgner and Herrmann, 2010). Current detailed models are limited to certain kinds of species. For example, the model from Ervens and Volkamer (2010) has been developed to study isoprene and its oxidation products like glyoxal. The CAPRAM 3.0i mechanism used by Tilgner and Herrmann (2010) is currently the most detailed aqueous phase organic chemistry model, taking into account the dissolution and aqueous chemistry of inorganic species and organic species up to four carbon atoms. However, atmospheric processing of long chain hydrocarbons is also expected to lead to the production of highly water soluble multifunctional organics in a few oxidation steps (e.g. van Pinxteren et al., 2005; Mazzoleni et al., 2010).

## Explicit modeling of volatile organic compounds

C. Mouchel-Vallon et al.

[Title Page](#)

[Abstract](#)

[Introduction](#)

[Conclusions](#)

[References](#)

[Tables](#)

[Figures](#)

◀

▶

◀

▶

[Back](#)

[Close](#)

[Full Screen / Esc](#)

[Printer-friendly Version](#)

[Interactive Discussion](#)



This study aims at exploring the production of water soluble compounds from the gaseous oxidation of long chain hydrocarbons of atmospheric interest and the sensitivity of this dissolution to NO<sub>x</sub> levels. To our knowledge, no modeling tool is currently available to describe in details the multiphase oxidation of long chain hydrocarbons.

5 This study describes the first stage in the development of such a modeling tool and examines the phase partitioning of organic species produced during the gas phase oxidation of hydrocarbons. A fully explicit chemical mechanism is used to describe the oxidation of organics in the gas phase and their mass transfer to the aqueous phase.

10 The oxidation of three hydrocarbons of atmospheric interest (isoprene, octane and  $\alpha$ -pinene) is investigated for various NO<sub>x</sub> conditions. Two scenarios are considered with a liquid water content corresponding either to a cloud or to deliquescent particles. The simulated carbon budget and the composition of the gas and aqueous phase are explored in detail.

## 2 Modeling tools

### 15 2.1 Gas phase chemistry

Formation of SOA through aqueous phase oxidation involves water soluble species produced during the gaseous phase oxidation of volatile organic compounds (VOC) (Aumont et al., 2000). Candidate species are typically highly functionalized molecules produced during the multigenerational oxidation of the hydrocarbons emitted in the atmosphere. The number of species needed to describe explicitly this multigenerational oxidation increases exponentially with the size of the carbon skeleton of the parent compound (Aumont et al., 2005). For long chain species (C<sub>>5</sub>), explicit oxidation schemes involve a number of intermediates that far exceeds the size of chemical schemes that can be written manually. The Generator for Explicit Chemistry and Kinetics of Organics in the Atmosphere (GECKO-A) is a computer tool that was developed to overcome this difficulty (Aumont et al., 2005). GECKO-A generates gas phase chemical

[Title Page](#)[Abstract](#)[Introduction](#)[Conclusions](#)[References](#)[Tables](#)[Figures](#)[|◀](#)[▶|](#)[Back](#)[Close](#)[Full Screen / Esc](#)[Printer-friendly Version](#)[Interactive Discussion](#)

## Explicit modeling of volatile organic compounds

C. Mouchel-Vallon et al.

[Title Page](#)

[Abstract](#)

[Introduction](#)

[Conclusions](#)

[References](#)

[Tables](#)

[Figures](#)

◀

▶

◀

▶

[Back](#)

[Close](#)

[Full Screen / Esc](#)

[Printer-friendly Version](#)

[Interactive Discussion](#)



## 2.2 Phase transfer

For each water soluble species A, the mass transfer between the gas and the aqueous phase is treated in a time dependent sense:



where  $k_l$  ( $s^{-1}$ ) is the pseudo first order rate constant of the gas-particle mass transfer and  $H_A$  ( $M\text{ atm}^{-1}$ ) is the Henry's law coefficient for the species A. The rate constant  $k_l$  can be expressed as (Schwartz, 1986):

$$k_l = L k_T = L \left( \frac{r^2}{3D_g} + \frac{4r}{3v\alpha} \right)^{-1} \quad (3)$$

where  $r$  (cm) is the radius of the particles or the droplets,  $D_g$  ( $\text{cm}^2 \text{s}^{-1}$ ) is the gas diffusion coefficient,  $v$  ( $\text{cm s}^{-1}$ ) is the mean molecular speed and  $\alpha$  (dimensionless) is the mass accommodation coefficient. The diffusion coefficient  $D_g$  can be estimated by scaling from a known reference compound:

$$\frac{D_g}{D_{g,\text{ref}}} = \sqrt{\frac{M_{\text{ref}}}{M}} \quad (4)$$

where  $M$  ( $\text{g mol}^{-1}$ ) is the molar mass and ref subscripts denote values for a reference species. We used water as reference compound,  $D_{g,\text{H}_2\text{O}} = 0.214/\text{P cm}^2 \text{s}^{-1}$  in air at 298 K (Ivanov et al., 2007),  $P$  (atm) being the atmospheric pressure.  $H$  is taken from the literature when available, using the database compiled by Raventos-Duran et al. (2010) for ca. 600 species. The empirical group contribution method GROMHE was used to estimate unknown constants (Raventos-Duran et al., 2010). GROMHE is able

Title Page

Abstract

Introduction

Conclusions

References

Tables

Figures

◀

▶

◀

▶

Back

Close

Full Screen / Esc

Printer-friendly Version

Interactive Discussion



to estimate Henry's law constants at temperature  $T = 298$  K for every atmospherically relevant organic species. The temperature dependence of  $H$  is represented with the Van't Hoff equation:

$$H(T) = H(298) \times \exp\left(\frac{\Delta H_{\text{solv}}}{R} \left(\frac{1}{298} - \frac{1}{T}\right)\right) \quad (5)$$

- 5 The enthalpy of dissolution  $\Delta H_{\text{solv}}$  ( $\text{J mol}^{-1}$ ) is also taken from the literature when available.  $\Delta H_{\text{solv}}$  typically ranges from 10 to 100  $\text{kJ mol}^{-1}$  (Kuhne et al., 2005) and a value of 50  $\text{kJ mol}^{-1}$  was used as a default value in the model. The mass accommodation coefficient  $\alpha$  is very poorly documented (ca. 40 constants in the literature, Davidovits et al., 2011; Sander et al., 2011). To our knowledge, the only SAR available to estimate  
10  $\alpha$  was proposed by Davidovits et al. (1995) and Nathanson et al. (1996). However the performances of that method cannot be rigorously evaluated due to the lack of experimental data. This method has therefore not been implemented and when no data are available,  $\alpha$  is set to a default value of  $\alpha = 0.05$  (Davidovits et al., 2011).

In this version of the model devoted to examine the phase partitioning of organics  
15 produced during gas phase processing, the only reactions taken into account in water are:

- i. Hydration of carbonyls. Species bearing ketone or aldehyde moieties undergo hydration equilibrium once they are dissolved. Equilibrium constants are estimated using the SAR from Raventos-Duran et al. (2010).
- 20 ii. Dissociation of acids. Carboxylic acids undergo acid/base equilibrium in water. Acidity constant are estimated following recommendations from Perrin et al. (1981).

Species are therefore not further oxidized in water. In the model, the only sink for the dissolved organic matter is caused by the gas phase chemical pump that shifts the  
25 water/gas equilibrium. For very soluble species, gas phase oxidation becomes slow

<a href="#">Title Page</a>	
<a href="#">Abstract</a>	<a href="#">Introduction</a>
<a href="#">Conclusions</a>	<a href="#">References</a>
<a href="#">Tables</a>	<a href="#">Figures</a>
<a href="#"></a>	<a href="#"></a>
<a href="#"></a>	<a href="#"></a>
<a href="#">Back</a>	<a href="#">Close</a>
<a href="#">Full Screen / Esc</a>	
<a href="#">Printer-friendly Version</a>	
<a href="#">Interactive Discussion</a>	



and the species remain in the aqueous phase in a form that can be considered as “permanent” in this version of the model.

## 2.3 Initial conditions

The modeling framework described above has been applied to the generation of the detailed mechanisms for three species of atmospheric interest: isoprene, octane and  $\alpha$ -pinene. Table 1 gives the total number of species after the complete generation of these chemical schemes. The number of species in the aqueous phase is in the same order of magnitude as the number of species in the gas phase. The phase partitioning is considered for non radical species only, but gem-diols (carbonyl hydration) and carboxylates (acid dissociation) are newly formed in water. Some of these newly formed species are highly soluble and therefore are not transferred to the gas phase.

As initial condition, the initial concentration of the precursor and  $O_3$  were set to 10 ppb and 40 ppb, respectively. The simulations were run with constant environmental conditions. Temperature was fixed to 278 K. Photolysis frequencies were calculated for mid-latitude and for a solar zenith angle of 45° using TUV (Madronich and Flocke, 1997).  $NO_x$  concentrations were held constant and three scenarios were considered corresponding to low  $NO_x$  (0.1 ppb), intermediate  $NO_x$  (1 ppb) and high  $NO_x$  (10 ppb) conditions. Oxidation of the organic species was initiated by adding a constant OH source of  $10^7$  radicals  $cm^{-3} s^{-1}$ . In these conditions, depending on the parent hydrocarbon, organic oxidation can be driven by OH,  $O_3$  or both. In this model configuration, the contribution of OH (97 % of the total oxidation of the precursor) is one order of magnitude higher than the contribution of  $O_3$  (3 %) to the oxidation of isoprene; OH and  $O_3$  contribute comparably (61 % and 39 %, respectively) to the oxidation of  $\alpha$ -pinene; octane is only oxidized by OH.

[Title Page](#)[Abstract](#)[Introduction](#)[Conclusions](#)[References](#)[Tables](#)[Figures](#)[|◀](#)[▶|](#)[◀](#)[▶](#)[Back](#)[Close](#)[Full Screen / Esc](#)[Printer-friendly Version](#)[Interactive Discussion](#)

### 3 Results

#### 3.1 Carbon budget and liquid water content

Figure 1 shows the time evolution of the carbon atom ratio during the oxidation of isoprene, octane and  $\alpha$ -pinene. Simulations were performed for three liquid water conditions: without aqueous phase ( $L = 0$ ), with a water content representative of deliquescent aerosols ( $L = 10^{-12}$ , e.g. Engelhart et al., 2011) and for typical cloud conditions ( $L = 3 \times 10^{-7}$ , e.g. Seinfeld and Pandis, 2006). We assume that the particle and cloud droplet sizes are monodisperse, with particle radii of 0.1  $\mu\text{m}$  and 5  $\mu\text{m}$ , respectively. Simulations are shown for a  $\text{NO}_x$  concentration set to 1 ppb.

Physical time is not fully appropriate to describe the temporal evolution for simulations conducted under constant environmental conditions. The temporal evolution is examined below as a function of the number of lifetime  $N_\tau$  of the parent hydrocarbon defined as:

$$N_\tau = \frac{t}{\tau} = \ln \frac{C_0}{C(t)} \quad (6)$$

where  $t$  is the simulated (physical) time,  $\tau$  is the lifetime of the parent hydrocarbon,  $C_0$  and  $C(t)$  its concentration at  $t_0$  and  $t$ , respectively. For these simulations, lifetimes of isoprene,  $\alpha$ -pinene and octane were approximately 1 h, 1.5 h and 1 day, respectively.

Under dry conditions ( $L = 0$ ), isoprene is slowly oxidized into CO and  $\text{CO}_2$  through a multigenerational process involving the formation of successive gaseous secondary intermediates of higher oxidation state (see Fig. 1a). The carbon budget is not affected by the presence of an aqueous phase representative of deliquescent aerosols (not shown). Dissolved organic carbon accounts for less than 1 % of the carbon atom ratio. With such low water content, only the more soluble species contribute to the organic content of the aqueous phase, i.e. the more functionalized ones. The top 10 contributors to the aqueous phase composition are  $\text{C}_5$  species bearing 4 functional groups each. For  $L$  set to a cloud value (Fig. 1b), moderately soluble species contribute

[Title Page](#)

[Abstract](#)

[Introduction](#)

[Conclusions](#)

[References](#)

[Tables](#)

[Figures](#)

◀

▶

◀

▶

[Back](#)

[Close](#)

[Full Screen / Esc](#)

[Printer-friendly Version](#)

[Interactive Discussion](#)



**Explicit modeling of volatile organic compounds**

C. Mouchel-Vallon et al.

[Title Page](#)[Abstract](#)[Introduction](#)[Conclusions](#)[References](#)[Tables](#)[Figures](#)[◀](#)[▶](#)[◀](#)[▶](#)[Back](#)[Close](#)[Full Screen / Esc](#)[Printer-friendly Version](#)[Interactive Discussion](#)

<a href="#">Title Page</a>	
<a href="#">Abstract</a>	<a href="#">Introduction</a>
<a href="#">Conclusions</a>	<a href="#">References</a>
<a href="#">Tables</a>	<a href="#">Figures</a>
<a href="#">◀◀</a>	<a href="#">▶▶</a>
<a href="#">◀</a>	<a href="#">▶</a>
<a href="#">Back</a>	<a href="#">Close</a>
<a href="#">Full Screen / Esc</a>	
<a href="#">Printer-friendly Version</a>	
<a href="#">Interactive Discussion</a>	

of the initial carbon atoms are found in water (52 % on a carbon basis) at the end of the simulation. Similar to the octane oxidation simulation, cloud water acts in this version of the model as an inert reservoir and slows down the CO + CO<sub>2</sub> formation. The CO + CO<sub>2</sub> fraction at  $N_t = 20$  decreases from 18 % for the dry scenario to 11 % for the cloud scenario.

### 3.2 Carbon budget and NO<sub>x</sub> conditions

The Henry's law constant of an organic compound is linked to the functional groups on the carbon backbone as well as the length of the carbon skeleton (e.g. Raventos-Duran et al., 2010; Schwarzenbach et al., 2005). The nature and the number of organic moieties added to the carbon skeleton during atmospheric processing depend in particular on NO<sub>x</sub> concentration (e.g. Finlayson-Pitts and Pitts, 2000; Atkinson and Arey, 2003). Simulations were therefore conducted for various scenarios: low NO<sub>x</sub> conditions (0.1 ppb), intermediate NO<sub>x</sub> conditions (1 ppb) and high NO<sub>x</sub> conditions (10 ppb). Figure 2 shows the results of these simulations for isoprene, octane and  $\alpha$ -pinene with a water content corresponding to cloud conditions. Note that modifications of the NO<sub>x</sub> conditions also impact on the concentrations of OH, O<sub>3</sub> and NO<sub>3</sub>. The relative contribution of these oxidants to oxidation of the precursors depends generally on NO<sub>x</sub> levels, especially for isoprene and  $\alpha$ -pinene. However, for all NO<sub>x</sub> conditions explored here, OH drives the oxidation of isoprene and both OH and O<sub>3</sub> drive the oxidation  $\alpha$ -pinene during the first oxidation steps. Therefore, NO<sub>x</sub> concentrations have an impact on secondary organics speciation mostly through the fate of peroxy radicals, rather than the initiation reactions.

Figure 2 shows that the dissolved organic content tends to increase with decreasing NO<sub>x</sub> concentration. The carbon atom ratio in the various phases appears to be especially sensitive to NO<sub>x</sub> for isoprene simulation. For the 3 hydrocarbons examined in this study, the largest effects on carbon partitioning are seen at the lower NO<sub>x</sub> concentrations. At the end of the simulations, the fraction of dissolved aqueous carbon is increased by 39 % for isoprene, 23 % for octane and 23 % for  $\alpha$ -pinene, from the

intermediate to the low NO<sub>x</sub> scenario (Fig. 2a, d, g). The amount of dissolved organic carbon is reduced by 20 % when NO<sub>x</sub> concentration is switched from intermediate to high NO<sub>x</sub> conditions in the isoprene case (see Fig. 2b, c).

### 3.3 Functional groups in the gas and aqueous phase

- 5 Figure 3a shows the distribution of the organic moieties of the simulated secondary organics at  $N_t = 2$  for the isoprene oxidation. The distribution is given for gas and aqueous phases, for the three NO<sub>x</sub> scenarios and for  $L$  set to cloud conditions. Results are provided as the number of functional groups per carbon atom ratio  $R_{OF/C}$ , defined as:

$$10 R_{OF/C} = \frac{\sum_i n_i^{OF} C_i}{\sum_i n_i^C C_i} \quad (7)$$

where  $OF$  is a given organic function.  $C_i$  is the concentration of species  $i$  in the considered phase and  $n_i^{OF}$  or  $n_i^C$  are the number of organic function OF or carbon atoms in the species  $i$ , respectively. In the gas phase, the degree of substitution of the organics ranges from 28 % (low NO<sub>x</sub> scenario) to 38 % (high NO<sub>x</sub> scenario). The distribution is dominated by carbonyls for all NO<sub>x</sub> scenarios. The substitution degree is comparatively larger in the aqueous phase than in the gas phase and ranges from 45 % (low NO<sub>x</sub> scenario) to 64 % (high NO<sub>x</sub> scenario). The hydroxyl group is a major moiety in the aqueous phase (substitution degree in the 22–30 % range). Under low NO<sub>x</sub> conditions, the organic peroxy radical chemistry is dominated by RO<sub>2</sub> + HO<sub>2</sub> reactions, leading to the formation of hydroperoxides ROOH. These hydroperoxides are major contributors to the aqueous phase organic content. Under high NO<sub>x</sub> conditions, the reaction RO<sub>2</sub> + NO dominates the evolution of peroxy radicals, leading among other things to the formation of the nitrate moiety. As expected, switching from low NO<sub>x</sub> to high NO<sub>x</sub>

<a href="#">Title Page</a>	
<a href="#">Abstract</a>	<a href="#">Introduction</a>
<a href="#">Conclusions</a>	<a href="#">References</a>
<a href="#">Tables</a>	<a href="#">Figures</a>
<a href="#">◀</a>	<a href="#">▶</a>
<a href="#">◀</a>	<a href="#">▶</a>
<a href="#">Back</a>	<a href="#">Close</a>
<a href="#">Full Screen / Esc</a>	
<a href="#">Printer-friendly Version</a>	
<a href="#">Interactive Discussion</a>	



## Explicit modeling of volatile organic compounds

C. Mouchel-Vallon et al.

[Title Page](#)

[Abstract](#)

[Introduction](#)

[Conclusions](#)

[References](#)

[Tables](#)

[Figures](#)

[◀](#)

[▶](#)

[◀](#)

[▶](#)

[Back](#)

[Close](#)

[Full Screen / Esc](#)

[Printer-friendly Version](#)

[Interactive Discussion](#)



conditions make the nitrate moiety grow at the expense of the hydroperoxide moiety (see Fig. 3a).

Figure 3b gives the distribution of organic species as a function chain length and the number of functional groups born by the molecules for the isoprene simulations at  $N_\tau = 2$ . The distribution is dominated by  $C_4$  species in the gas phase, mainly methyl vinyl ketone and methacrolein. In the aqueous phase, the distribution is dominated by  $C_5$  species bearing two functional groups, i.e. hydroxy-hydroperoxides species under low  $NO_x$  conditions and hydroxy-nitrate or hydroxy-nitrate or hydroxyl-carbonyl species under high  $NO_x$  conditions. Under high  $NO_x$  conditions, quadrifunctional  $C_5$  and  $C_4$  species contribute also substantially (11 %) to the organic content of the aqueous phase.

Figure 4 shows the distribution of organic moieties (panel a) and the distribution as a function of chain length and number of functional group (panel b) for the octane simulations at  $N_\tau = 2$ . The substitution degree ranges from 16–20 % in the gas phase to 31–33 % in the aqueous phase. The distribution is dominated by  $C_8$  species bearing one or two functional groups in the gas phase and two or three functional groups in the aqueous phase. The gas phase distribution is dominated by the carbonyl moieties, with a substantial contribution of nitrate moieties under high  $NO_x$  conditions. In the aqueous phase, about 21 % of the carbon atoms are substituted either by a hydroxy or a carbonyl moiety (see Fig. 4a). As expected, hydroperoxide is a significant functional group under low  $NO_x$  ( $R_{-OOH}/c = 7\%$ ) while nitrate is substantial under high  $NO_x$  ( $R_{-ONO_2}/c = 5\%$ ).

Figure 5 shows the distribution of the functional groups for the  $\alpha$ -pinene simulations. Molecules are functionalized with a substitution degree ranging from 16 % in the gas phase to 25 % in the aqueous phase. Difunctional  $C_{10}$  species dominate both the gas phase and the aqueous phase distribution (60 to 70 % of the carbon atom ratio in each phase). In the gas phase,  $C_9$  and  $C_8$  contribute substantially to the carbon budget (18–23 %). In the aqueous phase, trifunctional  $C_{10}$  contribute also substantially to the carbon budget (22–28 %). The gas phase is mainly composed of carbonyl compounds ( $R_{>CO}/c = 11\%$  under intermediate  $NO_x$  conditions). Nitrates

( $R_{\text{-ONO}_2/\text{C}} = 2.5\%$ ), hydroxy ( $R_{\text{-OH}/\text{C}} = 1.9\%$ ) and PAN ( $R_{\text{-CO(OONO}_2/\text{C}} = 2.3\%$ ) moieties contribute to a lesser extent to the gas phase composition. In the aqueous phase, the main contributors to the global functionalization are (hydrated) carbonyls ( $R_{>\text{CO}/\text{C}} + R_{\text{-C(OH)(OH)}/\text{C}} = 16\%$  under high  $\text{NO}_x$  conditions). The simulated substitution degree by carboxylic acids and their associated bases ( $R_{\text{-CO(OH)}/\text{C}} + R_{\text{-CO(O-)}}/\text{C}$ ) is 2.6 %. Nitrates are significant under high  $\text{NO}_x$  ( $R_{\text{-ONO}_2/\text{C}} = 4.4\%$ ) while hydroperoxydes have an important contribution under low  $\text{NO}_x$  conditions ( $R_{\text{-OOH}/\text{C}} = 4.5\%$ ).

### 3.4 Oxidative trajectories in an oxidation state vs. solubility framework

The gas phase oxidation of the organic species includes competitive processes leading either to the functionalization of the carbon backbone or to its fragmentation. The progressive functionalization of the carbon skeleton may lead to species with low enough volatility to condense. Conversely, fragmentation of the carbon skeleton leads to species with higher volatilities and ultimately to  $\text{CO}_2$ . In the context of organic partitioning between gas and aqueous phases, functionalization routes progressively increase the Henry's law coefficient of the species and therefore favor partitioning to the aqueous phase (e.g. Schwarzenbach et al., 2005; Raventos-Duran et al., 2010). The opposite behavior is usually noticed for the fragmentation routes. For example, Fig. 3 shows that for isoprene in all  $\text{NO}_x$  configurations, functionalized  $\text{C}_5$  species are mostly found in water whereas fragmented  $\text{C}_{<5}$  species tend to be preferentially found in the gas phase. Figure 4 (Fig. 5) shows that it is also true for octane ( $\alpha$ -pinene) where the proportion of functionalized  $\text{C}_8$  ( $\text{C}_{10}$ ) species is larger in the aqueous phase and the proportion of fragmented  $\text{C}_{<8}$  ( $\text{C}_{<10}$ ) species is larger in the gas phase.

Two dimensional frameworks have been recently proposed to examine the formation and aging of secondary organic aerosols during atmospheric oxidation of hydrocarbons (e.g. Jimenez et al., 2009; Pankow and Barsanti, 2009; Barsanti et al., 2011; Kroll et al., 2011). These frameworks attempt to capture the oxidative trajectories in a space defined by the volatility of the secondary species and their oxidation degree (e.g. Donahue et al., 2011, 2012). A similar two dimensional frameworks is used here to explore

[Title Page](#)[Abstract](#)[Introduction](#)[Conclusions](#)[References](#)[Tables](#)[Figures](#)[◀](#)[▶](#)[◀](#)[▶](#)[Back](#)[Close](#)[Full Screen / Esc](#)[Printer-friendly Version](#)[Interactive Discussion](#)

## Explicit modeling of volatile organic compounds

C. Mouchel-Vallon et al.

[Title Page](#)

[Abstract](#)

[Introduction](#)

[Conclusions](#)

[References](#)

[Tables](#)

[Figures](#)

◀

▶

◀

▶

[Back](#)

[Close](#)

[Full Screen / Esc](#)

[Printer-friendly Version](#)

[Interactive Discussion](#)

the oxidative trajectories in the context of a gas/aqueous multiphase system. We define the first dimension by the Henry's law coefficient  $H$ , used as a metric to represent the water solubility of the species. At thermodynamic equilibrium, the distribution of a species  $i$  between the gas and the aerosol phase is given by:

$$\xi^i = \frac{N_a^i}{N_a^i + N_g^i} = \left(1 + \frac{1}{H^i R T L}\right)^{-1} \quad (8)$$

where  $N_a^i$  and  $N_g^i$  (molec cm<sup>-3</sup> of air) are its number concentrations in the aqueous and gas phase, respectively. With  $L = 3 \times 10^{-7}$ , a species is equally distributed in the two phases ( $\xi = 0.5$ ) for  $H = 1.45 \times 10^5$  M atm<sup>-1</sup>. Species having  $H$  less than  $1.45 \times 10^3$  M atm<sup>-1</sup> will therefore almost exclusively be found in the gas phase ( $\xi < 0.01$ ), while species with  $H$  greater than  $1.45 \times 10^7$  M atm<sup>-1</sup> will almost exclusively be found in the aqueous phase ( $\xi > 0.99$ ). We use the mean carbon oxidation ( $\overline{OS}_C$ ) as the second dimension. In this framework, the parent hydrocarbon is placed at the bottom of the graph and the ending point of the oxidative trajectories ( $CO_2$ ) is placed at the top left ( $\overline{OS}_C = 4$ ).

Figure 6 shows the distribution of species produced during the gas phase oxidation of isoprene in this solubility/ $\overline{OS}_C$  space for 4 different times ( $N_\tau = 0, 1, 2, 10$ ). Distributions are shown for the 3 NO<sub>x</sub> scenarios. The carbon atom ratio of a given species is proportional to the volume of the bubble. Species contributing for less than 10<sup>-4</sup> to the total carbon are not shown for clarity. The SAR used to estimate  $H$  (Raventos-Duran et al., 2010) provides identical values for distinct position isomers. Position isomers with identical  $H$  are lumped to avoid overlap of the bubbles. In Fig. 6, species with a carbon backbone identical to the parent compound (blue bubbles) delineate the functionalization route. Species with a smaller backbone (orange bubbles) delineate trajectories including at least one fragmentation in the oxidation steps.

As expected, the first step of the isoprene oxidation is dominated by fragmentation routes (see Fig. 6). Under high NO<sub>x</sub> conditions, oxidation leads mostly to species with

---

**Explicit modeling of volatile organic compounds**

C. Mouchel-Vallon et al.

*H* in the  $10^0$ – $10^4$  M atm $^{-1}$  range, i.e. low enough to be mostly distributed in the gas phase at thermodynamic equilibrium. At  $N_\tau = 10$ , 10 species contribute for 90 % of the carbon budget. These species are the expected major isoprene oxidation products, as shown in Table 2. Under low NO<sub>x</sub> conditions, the solubility distribution spans more than

5 10 orders of magnitude. At  $N_\tau = 10$ , the carbon distribution is shifted to higher values of solubility. Therefore, the carbon atom fraction in the aqueous phase is substantial, reaching 63 % at  $N_\tau = 10$  (see Fig. 2i). The major contributors to the aqueous organic composition are an hydroxy-hydroperoxyde ( $\text{CH}_3\text{C}(\text{OOH})(\text{CH}_2(\text{OH}))\text{CH}=\text{CH}_2$ ) and its position isomers.

10 Figure 7 shows that the octane oxidation is first dominated by the functionalization routes and as oxidation proceeds fragmentation routes become substantial. Species are distributed in a broader range of solubility, at first in the  $10^{-3}$ – $10^8$  M atm $^{-1}$  range and then in the  $10^1$ – $10^{12}$  M atm $^{-1}$  range after the first oxidation steps. Thus species are at first evenly distributed in both phases and become more prevalent in the aqueous

15 phase after  $N_\tau = 2$  (see also Fig. 2). At  $N_\tau = 10$ , 60 % of the gaseous carbon can be ascribed to 10 species, peroxy acetyl nitrate and peroxy propyl nitrate being the major species, as seen in Table 2. Under low NO<sub>x</sub> conditions, the solubility distribution range is approximately the same, but more species are on the high solubility range ( $H > 7 \times 10^6$  M atm $^{-1}$ ). The fraction of dissolved carbon reaches 77 % at  $N_\tau = 10$ .

20 Like isoprene,  $\alpha$ -pinene oxidation is dominated by fragmentation (see Fig. 8).  $H$  values for most species fall in the  $10^5$ – $10^{13}$  M atm $^{-1}$  range, i.e. partition in the aqueous phase at thermodynamic equilibrium. In the gas phase, a difunctional C<sub>10</sub> PAN-like species is dominant, followed by acetone, formaldehyde and PAN (see Table 2). As expected from the species solubility range, dissolved carbon represents 71 % of the total carbon in low NO<sub>x</sub> conditions at  $N_\tau = 10$ .

---

<a href="#">Title Page</a>	
<a href="#">Abstract</a>	<a href="#">Introduction</a>
<a href="#">Conclusions</a>	<a href="#">References</a>
<a href="#">Tables</a>	<a href="#">Figures</a>
<a href="#"></a>	<a href="#"></a>
<a href="#"></a>	<a href="#"></a>
<a href="#">Back</a>	<a href="#">Close</a>
<a href="#">Full Screen / Esc</a>	
<a href="#">Printer-friendly Version</a>	
<a href="#">Interactive Discussion</a>	

---



## 4 Conclusions

Explicit gaseous oxidation schemes have been generated for three precursors of atmospheric interest (isoprene, octane,  $\alpha$ -pinene) using GECKO-A. The partitioning of the secondary organic compounds between gaseous and aqueous phases has been examined for a liquid water content corresponding to clouds and deliquescent aerosols. For  $L = 1 \times 10^{-12}$  (i.e. aerosols water), only a small fraction of the secondary organic carbon is influenced by the aqueous phase. For  $L = 3 \times 10^{-7}$  (i.e. cloud water), the phase distribution of organic carbon is sensitive to  $\text{NO}_x$  concentrations. For low  $\text{NO}_x$  conditions, 50 % (isoprene oxidation) to 70 % (octane oxidation) of the carbon atoms are found in the aqueous phase after the removal of the parent compound ( $N_\tau \approx 3$ ). For high  $\text{NO}_x$  condition, this ratio is only 5 % in the isoprene oxidation case, but remains large for  $\alpha$ -pinene and octane oxidation cases (40 % and 60 %, respectively). This study therefore suggests that most secondary organic species produced during the multigenerational oxidation of anthropogenic and biogenic hydrocarbons should dissolve in the aqueous phase during cloud events.

The simulated oxidative trajectories are examined in a new two dimensional space defined by the mean oxidation state and the water solubility. Isoprene oxidation is dominated by fragmentation routes. The solubility distribution of the isoprene oxidation products appears to be especially sensitive to  $\text{NO}_x$ , with low  $\text{NO}_x$  conditions favoring the production of more water soluble species. As a result, the fraction of dissolved carbon decreases from low to high  $\text{NO}_x$  conditions. Octane oxidation is first dominated by functionalization routes, next by fragmentation routes, producing highly soluble species in both low  $\text{NO}_x$  and high  $\text{NO}_x$  conditions. The fragmentation routes dominate the  $\alpha$ -pinene oxidation pathways and lead to highly water soluble species whatever the  $\text{NO}_x$  conditions are.

Once dissolved, organic species follow complex oxidation mechanisms. This study shows that during cloud events, a large fraction of organic matter could be processed in the aqueous phase and modify both the rates of reaction and the identity of their

<a href="#">Title Page</a>	
<a href="#">Abstract</a>	<a href="#">Introduction</a>
<a href="#">Conclusions</a>	<a href="#">References</a>
<a href="#">Tables</a>	<a href="#">Figures</a>
<a href="#"></a>	<a href="#"></a>
<a href="#"></a>	<a href="#"></a>
<a href="#">Back</a>	<a href="#">Close</a>
<a href="#">Full Screen / Esc</a>	
<a href="#">Printer-friendly Version</a>	
<a href="#">Interactive Discussion</a>	



products. To the best of our knowledge, this process is currently ignored in current atmospheric chemical models dealing with the oxidation of long chain organics. To explore the contribution of these cloud processes, aqueous oxidation mechanisms are needed for the very large set of species expected to be significantly dissolved in the cloud droplets. Protocols are required to generate consistent and comprehensive aqueous oxidation schemes on a systematic basis. This is the object of ongoing studies.

**Acknowledgements.** This work was funded by the French-German Joint Research Program in Atmospheric Chemistry.

10



The publication of this article is financed by CNRS-INSU.

## References

- Altieri, K. E., Seitzinger, S. P., Carlton, A. G., Turpin, B. J., Klein, G. C., and Marshall, A. G.: Oligomers formed through in-cloud methylglyoxal reactions: chemical composition, properties, and mechanisms investigated by ultra-high resolution FT-ICR mass spectrometry, *Atmos. Environ.*, 42, 1476–1490, 2008.
- Atkinson, R. and Arey, J.: Atmospheric degradation of volatile organic compounds, *Chem. Rev.*, 103, 4605–4638, 2003.
- Aumont, B., Madronich, S., Bey, I., and Tyndall G. S.: Contribution of secondary voc to the composition of aqueous atmospheric particles: a modeling approach, *J. Atmos. Chem.*, 35, 59–75, 2000.

15

20

<a href="#">Title Page</a>	
<a href="#">Abstract</a>	<a href="#">Introduction</a>
<a href="#">Conclusions</a>	<a href="#">References</a>
<a href="#">Tables</a>	<a href="#">Figures</a>
<a href="#"></a>	<a href="#"></a>
<a href="#"></a>	<a href="#"></a>
<a href="#">Full Screen / Esc</a>	
<a href="#">Printer-friendly Version</a>	
<a href="#">Interactive Discussion</a>	

- Aumont, B., Szopa, S., and Madronich, S.: Modelling the evolution of organic carbon during its gas-phase tropospheric oxidation: development of an explicit model based on a self generating approach, *Atmos. Chem. Phys.*, 5, 2497–2517, doi:10.5194/acp-5-2497-2005, 2005.
- 5 Aumont, B., Valorso, R., Mouchel-Vallon, C., Camredon, M., Lee-Taylor, J., and Madronich, S.: Modeling SOA formation from the oxidation of intermediate volatility *n*-alkanes, *Atmos. Chem. Phys.*, 12, 7577–7589, doi:10.5194/acp-12-7577-2012, 2012.
- Barth, M. C., Sillman, S., Hudman, R., Jacobson, M. Z., Kim, C. H., Monod, A., and Liang, J.: Summary of the cloud chemistry modeling intercomparison: photochemical box model simulation, *J. Geophys. Res.-Atmos.*, 108, 4214, doi:10.1029/2002JD002673, 2003.
- 10 Barsanti, K. C., Smith, J. N., and Pankow, J. F.: Application of the np plus mP modeling approach for simulating secondary organic particulate matter formation from alpha-pinene oxidation, *Atmos. Environ.*, 45, 6812–6819, 2011.
- Bateman, A. P., Nizkorodov, S. A., Laskin, J., and Laskin, A.: Photolytic processing of secondary organic aerosols dissolved in cloud droplets, *Phys. Chem. Chem. Phys.*, 13, 12199–12212, 15 2011.
- Camredon, M., Aumont, B., Lee-Taylor, J., and Madronich, S.: The SOA/VOC/NO<sub>x</sub> system: an explicit model of secondary organic aerosol formation, *Atmos. Chem. Phys.*, 7, 5599–5610, doi:10.5194/acp-7-5599-2007, 2007.
- Carlton, A. G., Wiedinmyer, C., and Kroll, J. H.: A review of Secondary Organic Aerosol (SOA) formation from isoprene, *Atmos. Chem. Phys.*, 9, 4987–5005, doi:10.5194/acp-9-4987-2009, 20 2009.
- Crahan, K. K., Hegg, D., Covert, D. S., and Jonsson, H.: An exploration of aqueous oxalic acid production in the coastal marine atmosphere, *Atmos. Environ.*, 38, 3757–3764, 2004.
- Davidovits, P., Hu, J. H., Worsnop, D. R., Zahniser, M. S., and Kolb, C. E.: Entry of gas molecules 25 into liquids, *Faraday Discuss.*, 100, 65–81, 1995.
- Davidovits, P., Kolb, C. E., Williams, L. R., Jayne, J. T., and Worsnop, D. R.: Update 1 of: mass accommodation and chemical reactions at gas–liquid interfaces, *Chem. Rev.*, 111, PR76–PR109, 2011.
- 30 Donahue, N. M., Epstein, S. A., Pandis, S. N., and Robinson, A. L.: A two-dimensional volatility basis set: 1. organic-aerosol mixing thermodynamics, *Atmos. Chem. Phys.*, 11, 3303–3318, doi:10.5194/acp-11-3303-2011, 2011.

[Title Page](#)[Abstract](#)[Introduction](#)[Conclusions](#)[References](#)[Tables](#)[Figures](#)[◀](#)[▶](#)[◀](#)[▶](#)[Back](#)[Close](#)[Full Screen / Esc](#)[Printer-friendly Version](#)[Interactive Discussion](#)

**Explicit modeling of volatile organic compounds**

C. Mouchel-Vallon et al.

Donahue, N. M., Kroll, J. H., Pandis, S. N., and Robinson, A. L.: A two-dimensional volatility basis set – Part 2: Diagnostics of organic-aerosol evolution, *Atmos. Chem. Phys.*, 12, 615–634, doi:10.5194/acp-12-615-2012, 2012.

El Haddad, I., Yao Liu, Nieto-Gligorovski, L., Michaud, V., Temime-Roussel, B., Quivet, E., Marchand, N., Sellegrí, K., and Monod, A.: In-cloud processes of methacrolein under simulated conditions – Part 2: Formation of secondary organic aerosol, *Atmos. Chem. Phys.*, 9, 5107–5117, doi:10.5194/acp-9-5107-2009, 2009.

Engelhart, G. J., Hildebrandt, L., Kostenidou, E., Mihalopoulos, N., Donahue, N. M., and Pandis, S. N.: Water content of aged aerosol, *Atmos. Chem. Phys.*, 11, 911–920, doi:10.5194/acp-11-911-2011, 2011.

Ervens, B., Carlton, A. G., Turpin, B. J., Altieri, K. E., Kreidenweis, S. M., and Feingold, G.: Secondary organic aerosol yields from cloud-processing of isoprene oxidation products, *Geophys. Res. Lett.*, 35, L02816, doi:10.1029/2007GL031828, 2008.

Ervens, B. and Volkamer, R.: Glyoxal processing by aerosol multiphase chemistry: towards a kinetic modeling framework of secondary organic aerosol formation in aqueous particles, *Atmos. Chem. Phys.*, 10, 8219–8244, doi:10.5194/acp-10-8219-2010, 2010.

Ervens, B., Turpin, B. J., and Weber, R. J.: Secondary organic aerosol formation in cloud droplets and aqueous particles (aqSOA): a review of laboratory, field and model studies, *Atmos. Chem. Phys.*, 11, 11069–11102, doi:10.5194/acp-11-11069-2011, 2011.

Finlayson-Pitts, B. J. and Pitts, J. N.: *Chemistry of the Upper and Lower Atmosphere*, Academic Press, San Diego, 2000.

Fu, T., Jacob, D. J., and Heald, C. L.: Aqueous-phase reactive uptake of dicarbonyls as a source of organic aerosol over Eastern North America, *Atmos. Environ.*, 43, 1814–1822, 2009.

Hallquist, M., Wenger, J. C., Baltensperger, U., Rudich, Y., Simpson, D., Claeys, M., Dommen, J., Donahue, N. M., George, C., Goldstein, A. H., Hamilton, J. F., Herrmann, H., Hoffmann, T., Iinuma, Y., Jang, M., Jenkin, M. E., Jimenez, J. L., Kiendler-Scharr, A., Maenhaut, W., McFiggans, G., Mentel, Th. F., Monod, A., Prévôt, A. S. H., Seinfeld, J. H., Suratt, J. D., Szmigielski, R., and Wildt, J.: The formation, properties and impact of secondary organic aerosol: current and emerging issues, *Atmos. Chem. Phys.*, 9, 5155–5236, doi:10.5194/acp-9-5155-2009, 2009.

Herrmann, H.: Kinetics of aqueous phase reactions relevant for atmospheric chemistry, *Chem. Rev.*, 103, 4691–4716, 2003.

<a href="#">Title Page</a>	
<a href="#">Abstract</a>	<a href="#">Introduction</a>
<a href="#">Conclusions</a>	<a href="#">References</a>
<a href="#">Tables</a>	<a href="#">Figures</a>
<a href="#"></a>	<a href="#"></a>
<a href="#"></a>	<a href="#"></a>
<a href="#">Back</a>	<a href="#">Close</a>
<a href="#">Full Screen / Esc</a>	
<a href="#">Printer-friendly Version</a>	
<a href="#">Interactive Discussion</a>	



**Explicit modeling of volatile organic compounds**

C. Mouchel-Vallon et al.

- Herrmann, H., Wolke, R., Muller, K., Bruggemann, E., Gnauk, T., Barzaghi, P., Mertes, S., Lehmann, K., Massling, A., Birmili, W., Wiedensohler, A., Wierprecht, W., Acker, K., Jaeschke, W., Kramberger, H., Svcina, B., Bachmann, K., Collett, J. L., Galgon, D., Schwirn, K., Nowak, A., van Pinxteren, D., Plewka, A., Chemnitzer, R., Rud, C., Hofmann, D., Tilgner, A., Diehl, K., Heinold, B., Hinneburg, D., Knoth, O., Sehili, A. M., Simmel, M., Wurzler, S., Majdik, Z., Mauersberger, G., and Muller, F.: Febuko and modmep: field measurements and modelling of aerosol and cloud multiphase processes, *Atmos. Environ.*, 39, 4169–4183, 2005.
- Ivanov, A. V., Trakhtenberg, S., Bertram, A. K., Gershenson, Y. M., and Molina, M. J.: OH, HO<sub>2</sub>, and ozone gaseous diffusion coefficients, *J. Phys. Chem. A*, 111, 1632–1637, 2007.
- Jacob, D. J.: Chemistry of oh in remote clouds and its role in the production of formic-acid and peroxymonosulfate, *J. Geophys. Res.-Atmos.*, 91, 9807–9826, 1986.
- Jimenez, J. L., Canagaratna, M. R., Donahue, N. M., Prevot, A. S. H., Zhang, Q., Kroll, J. H., DeCarlo, P. F., Allan, J. D., Coe, H., Ng, N. L., Aiken, A. C., Docherty, K. S., Ulbrich, I. M., Grieshop, A. P., Robinson, A. L., Duplissy, J., Smith, J. D., Wilson, K. R., Lanz, V. A., Hueglin, C., Sun, Y. L., Tian, J., Laaksonen, A., Raatikainen, T., Rautiainen, J., Vaattovaara, P., Ehn, M., Kulmala, M., Tomlinson, J. M., Collins, D. R., Cubison, M. J., Dunlea, E. J., Huffman, J. A., Onasch, T. B., Alfarra, M. R., Williams, P. I., Bower, K., Kondo, Y., Schneider, J., Drewnick, F., Borrmann, S., Weimer, S., Demerjian, K., Salcedo, D., Cottrell, L., Griffin, R., Takami, A., Miyoshi, T., Hatakeyama, S., Shimono, A., Sun, J. Y., Zhang, Y. M., Dzepina, K., Kimmel, J. R., Sueper, D., Jayne, J. T., Herndon, S. C., Trimborn, A. M., Williams, L. R., Wood, E. C., Middlebrook, A. M., Kolb, C. E., Baltensperger, U., and Worsnop, D. R.: Evolution of organic aerosols in the atmosphere, *Science*, 326, 1525–1529, 2009.
- Jordan, C., Ziemann, P., Griffin, R., Lim, Y., Atkinson, R., and Arey, J.: Modeling soa formation from oh reactions with C<sub>8</sub>-C<sub>17</sub> n-alkanes, *Atmos. Environ.*, 42, 8015–8026, 2008.
- Kreidenweis, S. M., Walcek, C. J., Feingold, G., Gong, W. M., Jacobson, M. Z., Kim, C. H., Liu, X. H., Penner, J. E., Nenes, A., and Seinfeld, J. H.: Modification of aerosol mass and size distribution due to aqueous-phase SO<sub>2</sub> oxidation in clouds: comparisons of several models, *J. Geophys. Res.-Atmos.*, 108, L02816, doi:10.1029/2007GL031828, 2003.
- Kroll, J. H., Donahue, N. M., Jimenez, J. L., Kessler, S. H., Canagaratna, M. R., Wilson, K. R., Altieri, K. E., Mazzoleni, L. R., Wozniak, A. S., Bluhm, H., Mysak, E. R., Smith, J. D.,

<a href="#">Title Page</a>	
<a href="#">Abstract</a>	<a href="#">Introduction</a>
<a href="#">Conclusions</a>	<a href="#">References</a>
<a href="#">Tables</a>	<a href="#">Figures</a>
<a href="#"></a>	<a href="#"></a>
<a href="#"></a>	<a href="#"></a>
<a href="#">Full Screen / Esc</a>	
<a href="#">Printer-friendly Version</a>	
<a href="#">Interactive Discussion</a>	



**Explicit modeling of volatile organic compounds**

C. Mouchel-Vallon et al.

[Title Page](#)[Abstract](#)[Introduction](#)[Conclusions](#)[References](#)[Tables](#)[Figures](#)[Back](#)[Close](#)[Full Screen / Esc](#)[Printer-friendly Version](#)[Interactive Discussion](#)

- Myriokefalitakis, S., Tsigaridis, K., Mihalopoulos, N., Sciare, J., Nenes, A., Kawamura, K., Segers, A., and Kanakidou, M.: In-cloud oxalate formation in the global troposphere: a 3-D modeling study, *Atmos. Chem. Phys.*, 11, 5761–5782, doi:10.5194/acp-11-5761-2011, 2011.
- Nathanson, G. M., Davidovits, P., Worsnop, D. R., and Kolb, C. E.: Dynamics and kinetics at the gas-liquid interface, *J. Phys. Chem.*, 100, 13007–13020, 1996.
- Nguyen, T. B., Roach, P. J., Laskin, J., Laskin, A., and Nizkorodov, S. A.: Effect of humidity on the composition of isoprene photooxidation secondary organic aerosol, *Atmos. Chem. Phys.*, 11, 6931–6944, doi:10.5194/acp-11-6931-2011, 2011.
- Pankow, J. F. and Barsanti, K. C.: The carbon number-polarity grid: a means to manage the complexity of the mix of organic compounds when modeling atmospheric organic particulate matter, *Atmos. Environ.*, 43, 2829–2835, 2009.
- Paulot, F., Crounse, J. D., Kjaergaard, H. G., Kroll, J. H., Seinfeld, J. H., and Wennberg, P. O.: Isoprene photooxidation: new insights into the production of acids and organic nitrates, *Atmos. Chem. Phys.*, 9, 1479–1501, doi:10.5194/acp-9-1479-2009, 2009a.
- Paulot, F., Crounse, J. D., Kjaergaard, H. G., Kurten, A., St Clair, J. M., Seinfeld, J. H., and Wennberg, P. O.: Unexpected epoxide formation in the gas-phase photooxidation of isoprene, *Science*, 325, 730–733, 2009b.
- Perrin, D. D., Dempsey B., and Serjeant, E. P.:  $pK_a$  Prediction for Organic Acids and Bases, Chapman and Hall, London, 1981.
- van Pinxteren, D., Plewka, A., Hofmann, D., Muller, K., Kramberger, H., Svrčina, B., Bachmann, K., Jaeschke, W., Mertes, S., Collett, J. L., and Herrmann, H.: Schmucke hill cap cloud and valley stations aerosol characterization during febuko (II): organic compounds, *Atmos. Environ.*, 39, 4305–4320, 2005.
- Raventos-Duran, T., Camredon, M., Valorso, R., Mouchel-Vallon, C., and Aumont, B.: Structure-activity relationships to estimate the effective Henry's law constants of organics of atmospheric interest, *Atmos. Chem. Phys.*, 10, 7643–7654, doi:10.5194/acp-10-7643-2010, 2010.
- Ravishankara, A. R.: Heterogeneous and multiphase chemistry in the troposphere, *Science*, 276, 1058–1065, 1997.
- Russell, L. M., Bahadur, R., and Ziemann, P. J.: Identifying organic aerosol sources by comparing functional group composition in chamber and atmospheric particles, *Proc. Natl. Acad. Sci. USA*, 108, 3516–3521, 2011.

## Explicit modeling of volatile organic compounds

C. Mouchel-Vallon et al.

[Title Page](#)[Abstract](#)[Introduction](#)[Conclusions](#)[References](#)[Tables](#)[Figures](#)[Back](#)[Close](#)[Full Screen / Esc](#)[Printer-friendly Version](#)[Interactive Discussion](#)

- Sander, S. P., Abbatt, J., Barker, J. R., Burkholder, J. B., Friedl, R. R., Golden, D. M., Huie, R. E., Kolb, C. E., Kurylo, M. J., Moortgat, G. K., Orkin, V. L., and Wine, P. H.: Chemical kinetics and photochemical data for use in atmospheric studies, evaluation no. 17, JPL Publication, 10-6, Pasadena, California, 2011.
- 5 Schwartz, S. E.: Mass-transport considerations pertinent to aqueous phase reactions of gases in liquid-water clouds, NATO ASI Series, G6, 415–471, 1986.
- Schwarzenbach, R. P., Gschwend, P. M., and Imboden, D. M., Equilibrium partitioning between gaseous, liquid, and solid phases, in: Environmental Organic Chemistry, John Wiley & Sons, New York, 55–458, 2005.
- 10 Seinfeld, J. H. and Pandis, S. N.: Atmospheric Chemistry and Physics, From Air Pollution to Climate Change, John Wiley & Sons, New York, 2006.
- Sorooshian, A., Ng, N. L., Chan, A. W. H., Feingold, G., Flagan, R. C., and Seinfeld, J. H.: Particulate organic acids and overall water-soluble aerosol composition measurements from the 15 2006 gulf of mexico atmospheric composition and climate study (GOMACCS), *J. Geophys. Res.-Atmos.*, 112, D13201, doi:10.1029/2007JD008537, 2007.
- Tilgner, A. and Herrmann, H.: Radical-driven carbonyl-to-acid conversion and acid degradation in tropospheric aqueous systems studied by capram, *Atmos. Environ.*, 44, 5415–5422, 2010.
- Valorso, R., Aumont, B., Camredon, M., Raventos-Duran, T., Mouchel-Vallon, C., Ng, N. L., Seinfeld, J. H., Lee-Taylor, J., and Madronich, S.: Explicit modelling of SOA formation from 20  $\alpha$ -pinene photooxidation: sensitivity to vapour pressure estimation, *Atmos. Chem. Phys.*, 11, 6895–6910, doi:10.5194/acp-11-6895-2011, 2011.
- Warneck, P.: Multi-phase chemistry of C<sub>2</sub> and C<sub>3</sub> organic compounds in the marine atmosphere, *J. Atmos. Chem.*, 51, 119–159, 2005.
- Zhou, Y., Zhang, H., Parikh, H. M., Chen, E. H., Rattanavaraha, W., Rosen, E. P., Wang, W., and 25 Kamens, R. M.: Secondary organic aerosol formation from xylenes and mixtures of toluene and xylenes in an atmospheric urban hydrocarbon mixture: water and particle seed effects (ii), *Atmos. Environ.*, 45, 3882–3890, 2011.

[Title Page](#)[Abstract](#)[Introduction](#)[Conclusions](#)[References](#)[Tables](#)[Figures](#)[|◀](#)[▶|](#)[Back](#)[Close](#)[Full Screen / Esc](#)[Printer-friendly Version](#)[Interactive Discussion](#)

**Explicit modeling of volatile organic compounds**

C. Mouchel-Vallon et al.

**Table 1.** Number of species in the generated chemical mechanism.

Precursor species	Gas phase	Aqueous phase	Total
Isoprene	$5.9 \times 10^3$	$3.2 \times 10^3$	$9.1 \times 10^3$
Octane	$1.1 \times 10^5$	$5.0 \times 10^4$	$1.6 \times 10^5$
$\alpha$ -pinene	$3.2 \times 10^5$	$2.5 \times 10^5$	$5.6 \times 10^5$

[Title Page](#)[Abstract](#)[Introduction](#)[Conclusions](#)[References](#)[Tables](#)[Figures](#)[Back](#)[Close](#)[Full Screen / Esc](#)[Printer-friendly Version](#)[Interactive Discussion](#)

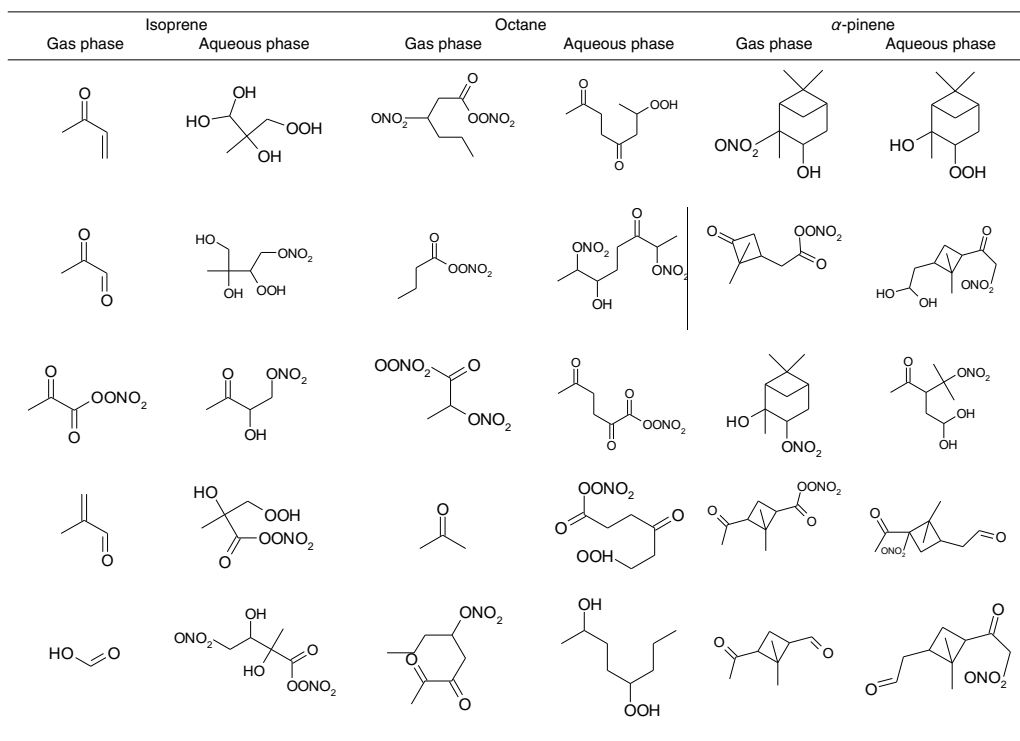
## Explicit modeling of volatile organic compounds

C. Mouchel-Vallon et al.

Gas phase	Isoprene Aqueous phase	Octane Gas phase	Aqueous phase	Gas phase	$\alpha$ -pinene Aqueous phase
HCHO					
				HCHO	
		HCHO			

<a href="#">Title Page</a>	<a href="#">Abstract</a>	<a href="#">Introduction</a>
<a href="#">Conclusions</a>	<a href="#">References</a>	
<a href="#">Tables</a>	<a href="#">Figures</a>	
<a href="#">◀</a>	<a href="#">▶</a>	
<a href="#">◀</a>	<a href="#">▶</a>	
<a href="#">Back</a>	<a href="#">Close</a>	
<a href="#">Full Screen / Esc</a>		
<a href="#">Printer-friendly Version</a>		
<a href="#">Interactive Discussion</a>		



**Table 2.** (Continued.)

## Explicit modeling of volatile organic compounds

C. Mouchel-Vallon et al.

- [Title Page](#)
- [Abstract](#) | [Introduction](#)
- [Conclusions](#) | [References](#)
- [Tables](#) | [Figures](#)
- [◀](#) | [▶](#)
- [◀](#) | [▶](#)
- [Back](#) | [Close](#)
- [Full Screen / Esc](#)
- [Printer-friendly Version](#)
- [Interactive Discussion](#)

## Explicit modeling of volatile organic compounds

C. Mouchel-Vallon et al.

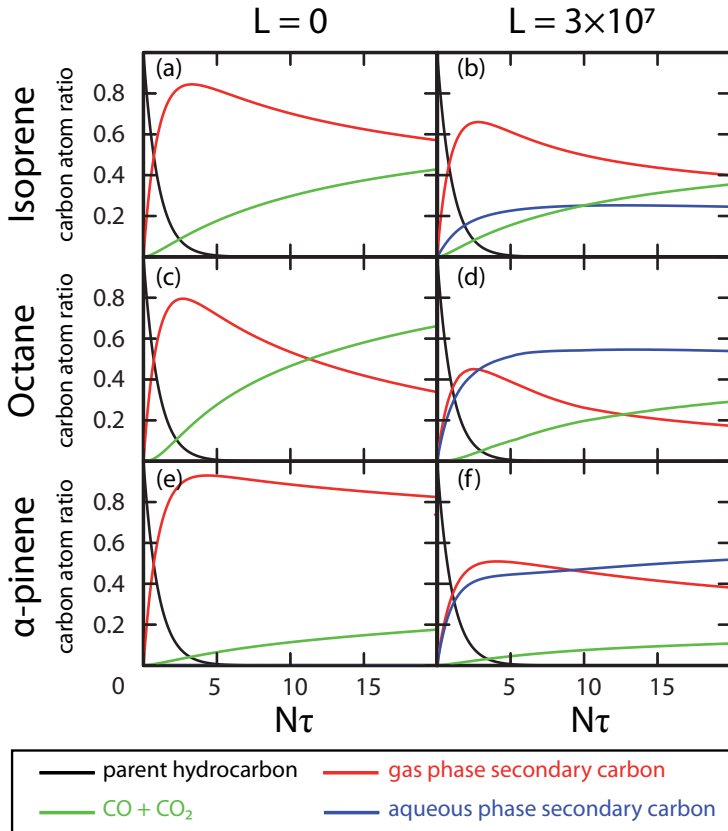


**Fig. 1.** Carbon budget during the oxidation of isoprene (top row), octane (middle row) and  $\alpha$ -pinene (bottom row) for liquid water content of 0 (1st column) and  $3 \times 10^{-7}$  (2nd column), under intermediate  $\text{NO}_x$  conditions ( $\text{NO}_x = 1 \text{ ppb}$ ). The time scale is defined as multiples of lifetimes of the initial hydrocarbon, as described in the text.

- [Title Page](#)
- [Abstract](#) | [Introduction](#)
- [Conclusions](#) | [References](#)
- [Tables](#) | [Figures](#)
- [◀](#) | [▶](#)
- [◀](#) | [▶](#)
- [Back](#) | [Close](#)
- [Full Screen / Esc](#)
- [Printer-friendly Version](#)
- [Interactive Discussion](#)



## Discussion Paper | Explicit modeling of volatile organic compounds

C. Mouchel-Vallon et al.

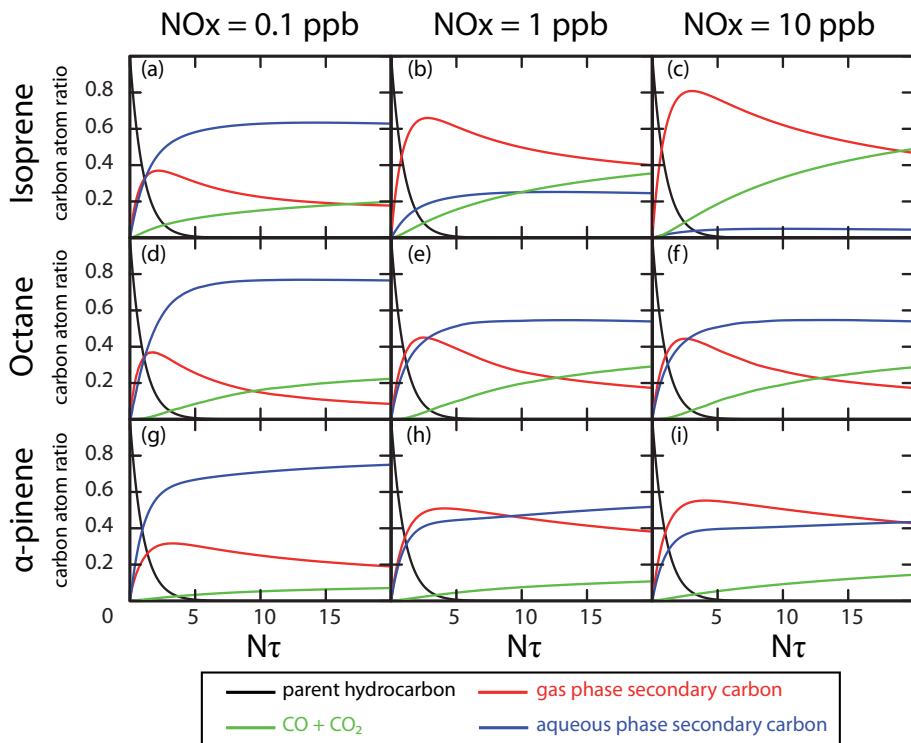


**Fig. 2.** Carbon budget during the oxidation of isoprene (top line), octane (middle line) and  $\alpha$ -pinene (bottom line) for a  $\text{NO}_x$  concentration of 0.1 ppb (1st column), 1 ppb (2nd column) and 10 ppb (3rd column), with a cloud liquid water content ( $L = 3 \times 10^{-7}$ ). The time scale is described in the text.

- [Title Page](#)
- [Abstract](#) | [Introduction](#)
- [Conclusions](#) | [References](#)
- [Tables](#) | [Figures](#)
- [◀](#) | [▶](#)
- [◀](#) | [▶](#)
- [Back](#) | [Close](#)
- [Full Screen / Esc](#)
- [Printer-friendly Version](#)
- [Interactive Discussion](#)

## Explicit modeling of volatile organic compounds

C. Mouchel-Vallon et al.

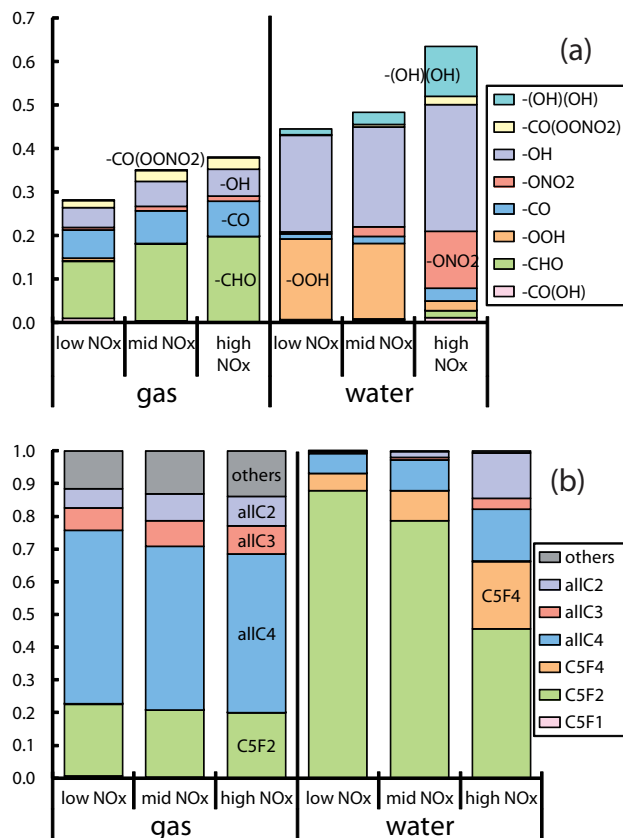


**Fig. 3.** At  $N_t = 2$ , simulated distribution in gaseous and aqueous phase of organic moieties ratio ( $R_{\text{OF/C}}$ , **a**) and functionalization (**b**) for a cloud water content during the oxidation of isoprene.  $CmFn$  category merges species with  $m$  carbon atoms bearing  $n$  functional groups. The precursor and C1 species are lumped in the *others* category.

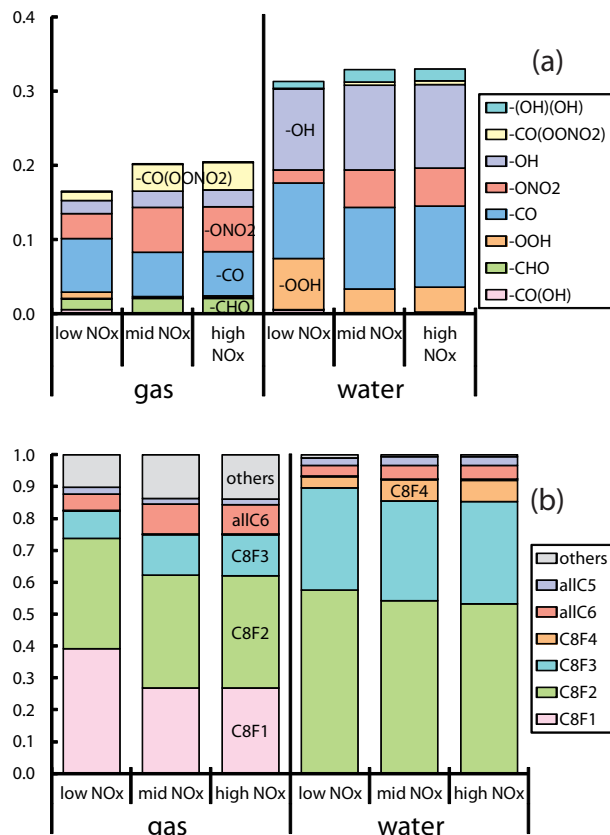


**Fig. 4.** At  $N_\tau = 2$ , simulated distribution in gaseous and aqueous phase of organic moieties ratio ( $R_{\text{OF/C}}$ , **a**) and functionalization (**b**) for a cloud water content during the oxidation of octane.  $\text{C}_m\text{Fn}$  category merges species with  $m$  carbon atoms bearing  $n$  functional groups. The precursor and C1–C4 species are lumped in the *others* category.

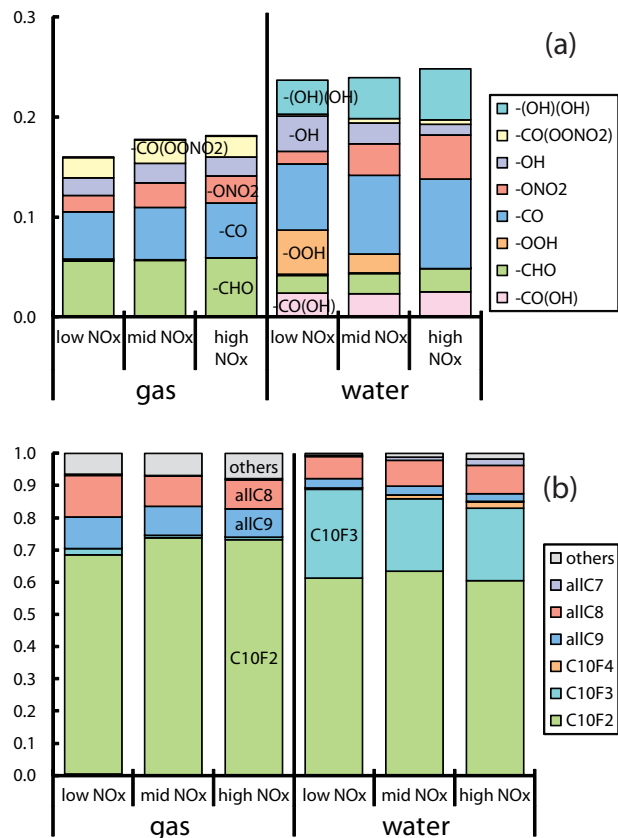


**Fig. 5.** At  $N_\tau = 2$ , simulated distribution in gaseous and aqueous phase of organic moieties ratio ( $R_{\text{OF/C}}$ , **a**) and functionalization (**b**) for a cloud water content during the oxidation of  $\alpha$ -pinene.  $CmFn$  category merges species with  $m$  carbon atoms bearing  $n$  functional groups. The precursor and C1–C6 species are lumped in the *others* category.

## Explicit modeling of volatile organic compounds

C. Mouchel-Vallon et al.

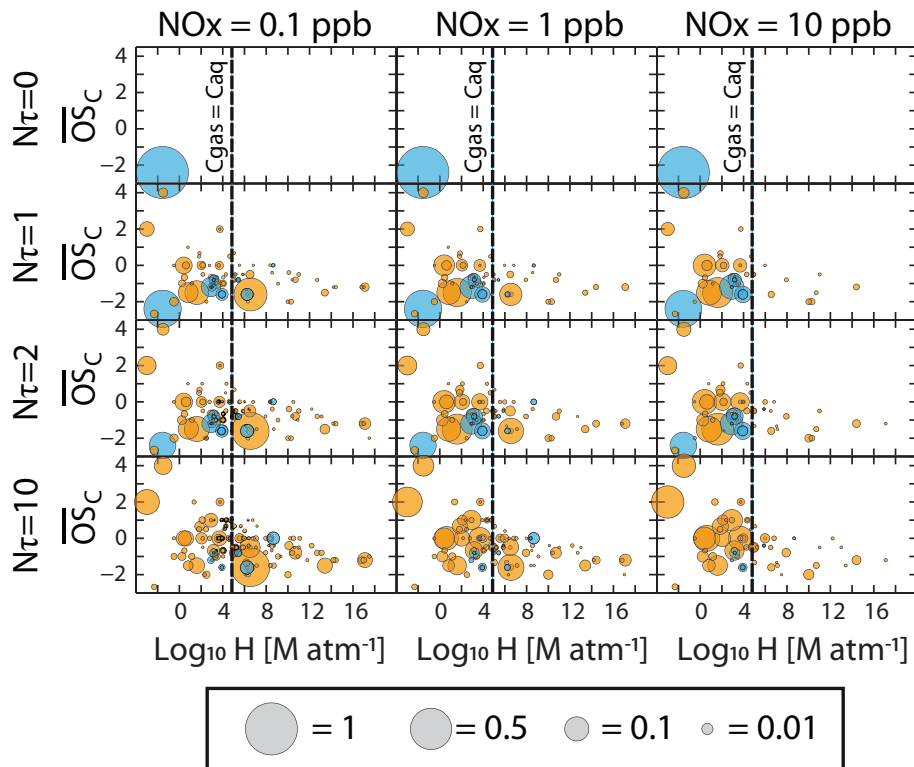


**Fig. 6.** Solubility and mean oxidation state of the species produced during the oxidation of isoprene under low  $\text{NO}_x$  (1st column), intermediate  $\text{NO}_x$  (2nd column) and high  $\text{NO}_x$  (3rd column) conditions as a function of the number of precursor lifetime. Contribution of a species to the global carbon budget is proportional to the volume of the bubble. Position isomers having identical volatility and oxidation state are lumped in the same bubble. Blue bubbles denote species having the carbon skeleton of the parent hydrocarbon. Orange bubbles denote species with less carbon atoms than the parent compound. The black dashed lines denote the solubility for which a compound is equally distributed in the aqueous and gaseous phases.

## Explicit modeling of volatile organic compounds

C. Mouchel-Vallon et al.

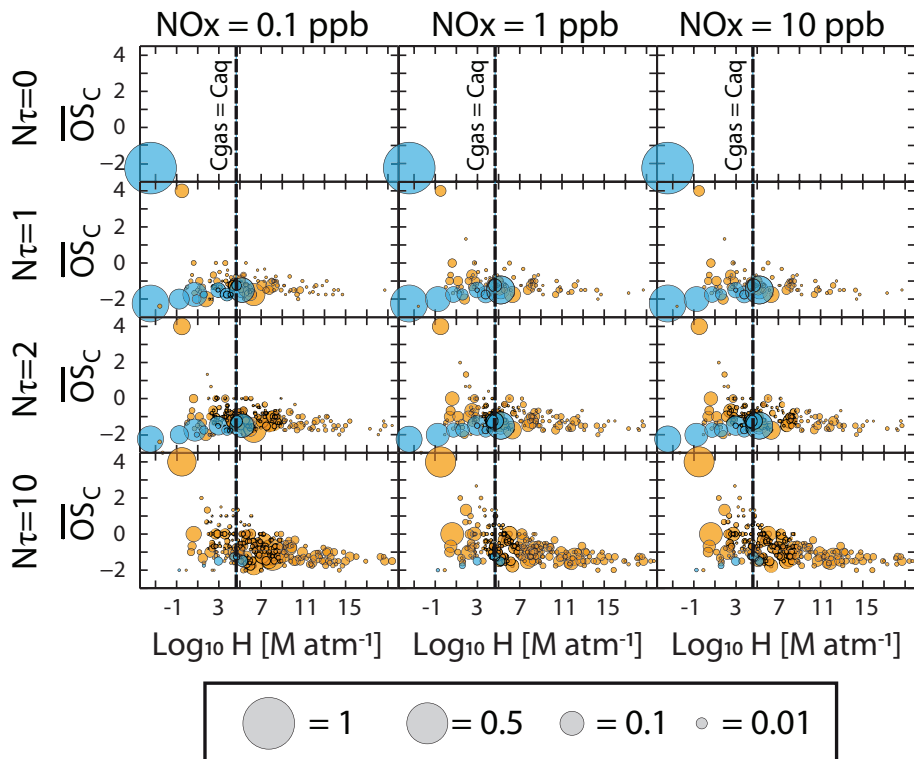


**Fig. 7.** Solubility and mean oxidation state of the species produced during the oxidation of octane under low  $\text{NO}_x$  (1st column), intermediate  $\text{NO}_x$  (2nd column) and high  $\text{NO}_x$  (3rd column) conditions as a function of the number of precursor lifetime. See Fig. 6 caption for the color code of the bubbles.

- [Title Page](#)
- [Abstract](#) | [Introduction](#)
- [Conclusions](#) | [References](#)
- [Tables](#) | [Figures](#)
- [◀](#) | [▶](#)
- [◀](#) | [▶](#)
- [Back](#) | [Close](#)
- [Full Screen / Esc](#)
- [Printer-friendly Version](#)
- [Interactive Discussion](#)

## Explicit modeling of volatile organic compounds

C. Mouchel-Vallon et al.

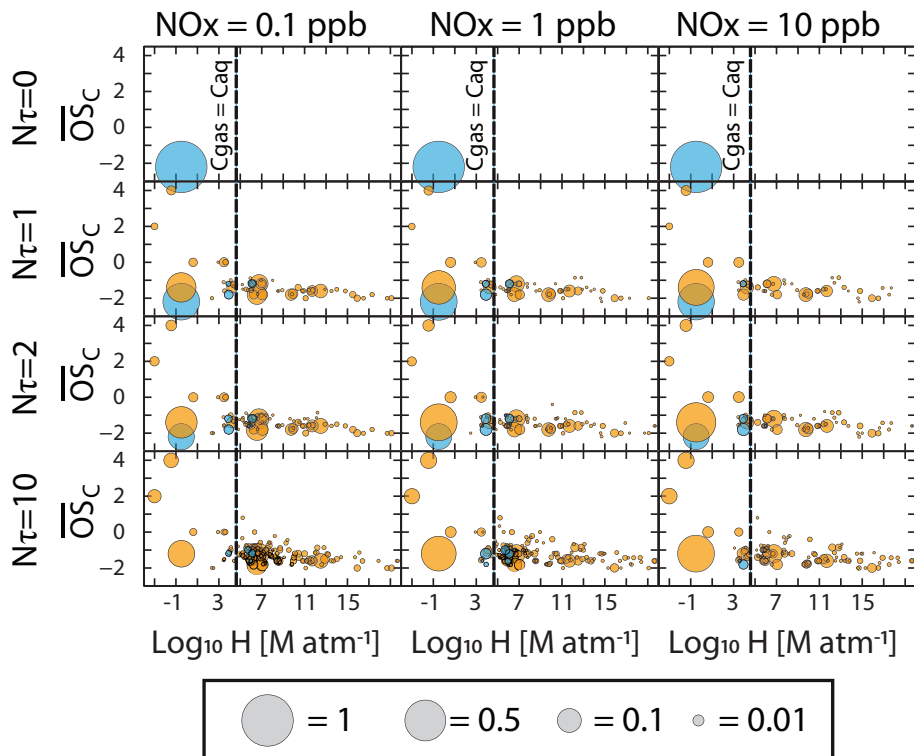


**Fig. 8.** Solubility and mean oxidation state of the species produced during the oxidation of  $\alpha$ -pinene under low  $\text{NO}_x$  (1st column), intermediate  $\text{NO}_x$  (2nd column) and high  $\text{NO}_x$  (3rd column) conditions as a function of the number of precursor lifetime. See Fig. 6 caption for the color code of the bubbles.

- [Title Page](#)
- [Abstract](#) | [Introduction](#)
- [Conclusions](#) | [References](#)
- [Tables](#) | [Figures](#)
- [◀](#) | [▶](#)
- [◀](#) | [▶](#)
- [Back](#) | [Close](#)
- [Full Screen / Esc](#)
- [Printer-friendly Version](#)
- [Interactive Discussion](#)

